Original Article

JCBFM

Journal of Cerebral Blood Flow & Metabolism
2022, Vol. 42(5) 757–770

DOI: 10.1177/0271678X21065391
journals.sagepub.com/home/jcbfm
SAGE

Oligodendrocyte precursor cell transplantation promotes angiogenesis and remyelination via Wnt/β-catenin pathway in a mouse model of middle cerebral artery occlusion

Li-Ping Wang[1,2], Jiaji Pan[2], Yongfang Li[2], Jieli Geng[1], Chang Liu[2], Lin-Yuan Zhang[2], Panting Zhou[2], Yao-Hui Tang[2], Yongting Wang[2], Zhijun Zhang[2] and Guo-Yuan Yang[2]

Abstract

White matter injury is a critical pathological characteristic during ischemic stroke. Oligodendrocyte precursor cells participate in white matter repairing and remodeling during ischemic brain injury. Since oligodendrocyte precursor cells could promote Wnt-dependent angiogenesis and migrate along vasculature for the myelination during the development in the central nervous system, we explore whether exogenous oligodendrocyte precursor cell transplantation promotes angiogenesis and remyelination after middle cerebral artery occlusion in mice. Here, oligodendrocyte precursor cell transplantation improved motor and cognitive function, and alleviated brain atrophy. Furthermore, oligodendrocyte precursor cell transplantation promoted functional angiogenesis, and increased myelin basic protein expression after ischemic stroke. The further study suggested that white matter repairing after oligodendrocyte precursor cell transplantation depended on angiogenesis induced by Wnt/β-catenin signal pathway. Our results demonstrated a novel pathway that Wnt7a from oligodendrocyte precursor cells acting on endothelial β-catenin promoted angiogenesis and improved neurobehavioral outcomes, which facilitated white matter repair and remodeling during ischemic stroke.

Keywords

Angiogenesis, ischemia, oligodendrocyte precursor cells, white matter, Wnt/β-catenin

Received 10 June 2021; Revised 20 October 2021; Accepted 19 November 2021

Introduction

Ischemic stroke is among the most common causes of death and disability in the world.[1,2] White matter injury is the canonical factor for the motor and cognition dysfunction after ischemic stroke. However, it has largely been neglected in animal studies and clinical trials. White matter is highly vulnerable to ischemia and accounts for half of the lesion volume in most cases of human stroke.[3,4] Clinical symptoms such as cognitive dysfunction, emotional disorders and sensorimotor impairments, are closely associated with the destruction of white matter connectivity.[5] Therefore, the protection of white matter from an ischemic brain injury should be paid more attention.[6]

White matter consists of axons, oligodendrocytes, and astrocytes. Axons are wrapped by myelin sheets, which is critical for the accuracy and speed of nerve signal conduction.[7] Oligodendrocytes are the myelinating cells responsible for axonal myelination and are

[1]Department of Neurology, Renji Hospital, Shanghai Jiao Tong University School of Medicine, Shanghai 200120, China
[2]Med-X Research Institute and School of Biomedical Engineering, Shanghai Jiao Tong University, Shanghai, China

Corresponding authors:
Guo-Yuan Yang, Med-X Research Institute and School of Biomedical Engineering, Shanghai Jiao Tong University, 1954 Hua Shan Road, Shanghai 200030, China. Email: gyyang@sjtu.edu.cn

Zhijun Zhang, Med-X Research Institute and School of Biomedical Engineering, Shanghai Jiao Tong University, 1954 Hua Shan Road, Shanghai 200030, China.
E-mail: zhangzj@sjtu.edu.cn

highly susceptible to damages.[8] Oligodendrocytes develop from oligodendrocyte precursor cells (OPCs) and OPCs mediate the remyelination process after brain injury.[9] Ischemic stroke induces endogenous oligodendrogenesis, which plays an important role in maintaining the structure and function of axons.[3] However, only a small amount of OPCs is capable to migrate to the ischemic region and differentiate into mature myelin.[3] Since postinjury endogenous remyelination is rarely complete, OPC transplantation is a potential treatment option.[8,10] OPC transplantation has been proved to promote remyelination in spinal cord injury and multiple sclerosis.[11,12] Transplanted OPCs showed potent white matter protective effects and enhanced spatial learning and memory after hypoxic ischemic injury in premature rat brain.[13] However, the molecular mechanism of re-myelination induced by OPC transplantation after ischemic stroke is obscure.

In our previous study, OPC transplantation could protect blood-brain barrier in the acute phase of ischemic stroke via activating Wnt/β-catenin pathway.[14] This pathway is involved in cellular proliferation, survival, differentiation, migration and apoptosis, and is associated with angiogenesis and vascular maturation in cancers and postnatal brain development.[15–18] Wnt7 is the ligand activating β-catenin in Wnt/β-catenin pathway and the paracrine Wnt7 of OPC promotes Wnt dependent angiogenesis.[16] Angiogenesis participates in brain plasticity and functional recovery during chronic phase of stroke.[19] Neovascularization increases cerebral blood flow, provides energy for OPC differentiation and myelination, and regulates OPC survival, proliferation and migration through paracrine.[20] Whether OPC transplantation could couple angiogenesis and remyelination in ischemic stroke by Wnt/β-catenin pathway is unclear.

In the present study, we use a mouse model of transient middle cerebral artery occlusion (tMCAO) to explore whether exogenous OPC transplantation promotes functional angiogenesis and white matter repairing for the functional recovery after ischemic brain injury.

Materials and methods

Animals

Animal experimental procedures were approved by the Institutional Animal Care and Use Committee (IACUC) of Shanghai Jiao Tong University, Shanghai, China. All studies were conducted in accordance with the US National Research Council's Guide for the Care and Use of Laboratory Animals, the US Public Health Service's Policy on Humane Care and Use of Laboratory Animals and Guide for the Care and Use of Laboratory Animals. Animal studies were reported according to ARRIVE 2.0 guidelines.[21] Adult male Institute of Cancer Research (ICR) mice (n = 108) weighing 28–30 g (Jeisijie, Shanghai, China) were randomly divided into 4 groups: sham group, phosphate buffered saline (PBS) treated group (as a control), OPC-treated group, and OPC-treated plus XAV-939 group, n = 25–28 per group (Suppl. 1e). Animals were housed with free access to water and food.

OPC isolation and identification

The brain cortex was dissected from P1 Sprague-Dawley rat pups as described.[22,23] Brain tissue was dissociated into a single-cell suspension by trypsinize at 37 °C for 10 min and the suspension was filtered with a 70-μm filter. The cells were seeded on poly-d-lysine (PDL, Sigma-Aldrich, San Louis, MO) coated culture flasks in DMEM (Corning, New York, NY) with 10% fatal calf serum (Gibco, Carlsbad, CA). Eight days later, the microglia were separated from glia cell mixtures after 30 min of culture by a 220 rpm shake. After 20 hours of culture by a 200 rpm shake, the cells were collected. Then OPCs were injected into the mice or seeded on a PDL coated culture dish in Neurobasal-A(Gibco) containing 2% B27 (Gibco), 10 ng/ml PDGF-AA (Gibco), 10 ng/ml bFGF (Peprotech, NJ, USA) and 2 mmol/l glutamine (Gibco).

Cells were identified by immunofluorescence staining of platelet-derived growth factor-α (PDGFR-α) and neuron-glial antigen 2 (NG2). Cells were fixed with 4% paraformaldehyde for 5 min at room temperature and blocked by 10% bovine serum albumin. Then OPCs were incubated with primary antibodies against PDGFR-α (1:100, Santa Cruz Biotechnology, Santa Cruz, CA), NG2 (1:200, Millipore, Bedford, MA), MBP (1:200, Abcam, MA), GAFP (1:500, Millipore), NeuN (1:200, Millipore) and Iba-1 (1:200, WAKO, Osaka, Japan) at 4 °C overnight. Cells were incubated with the fluorescence conjugated second antibodies for 1 hour at room temperature.

A model of tMCAO in mouse

The mouse MCAO was described previously.[24,25] Briefly, mice were anesthetized by 1.5% isoflurane (RWD Life Science, Shenzhen, China). After the isolation of the left common carotid artery, external and internal carotid arteries, the origin of middle cerebral artery was occluded by a silicone-coated 6-0 suture (Covidien, Mansfield, MA). The suture was withdrawn after 90 min of tMCAO. To confirm the successful occlusion and reperfusion, cerebral blood flow was measured by a laser Doppler flowmetry (Moor Instruments, Devon, UK). The success of occlusion

was assessed by a decrease of cerebral blood flow at least 80% of the baseline. Body temperature was maintained at $37 \pm 0.2\,^{\circ}C$ throughout the surgery using a heating pad (RWD Life Science). Sham mice were conducted the same procedure except the insertion of suture.

OPC transplantation

Animals after tMCAO were randomly divided into OPC treated mice or PBS treated mice (as a control). OPCs or PBS were injected at 24 hours after tMCAO. Before transplantation, OPCs were labeled with carboxyfluorescein diacetate-succinimidyl ester (CFDA-SE, Beyotime, Shanghai, China) for tracking. An amount of 6×10^5 OPCs was suspected in 5 µl PBS and slowly injected into the left striatum at 2 mm lateral to the bregma and 3 mm under the dura (AP = 0 mm, ML = 2 mm, DV = 3 mm) at a rate of 1 µl/min by the 10 µl Hamilton syringe (Hamilton, Bonaduz, Switzerland).[14,25] The same amount of PBS was injected as control. The mice were injected i.p. daily with cyclosporine A (5 mg/kg, Sigma) for immunosuppression after cell transplantation.

Administration of β-catenin inhibitor

The β-catenin inhibitor, XAV-939 (40 mg/kg, MCE, Monmouth Junction, NJ), was injected intraperitoneally once per day after OPC transplantation for 13 days.

Neurobehavioral tests

The modified neurological severity score (mNSS) was performed by an investigator who was blinded to the experimental treatment to evaluate the neurological function at 7 and 14 days after tMCAO. The mNSS ranged from 0 to 14 and included motor, sensory, balance and reflex tests.[26]

To test the motor function, rotarod test was performed at 7 and 14 days after tMCAO. Briefly, mice were trained on a rotating rod at 20 rpm for 3 consecutive days before tMCAO. At the test day, the rod was continuously accelerated to 40 rpm and the time mice stayed on the rod (latency to fall) was recorded.

To test the cognitive function, fear conditioning test and step through test were performed at 14 days after tMCAO.

Fear conditioning test was performed at 14 days after tMCAO. At the first day of the test, a mouse was put into the cage with an electric stimulator at the base (AfaSci Research Laboratories, Redwood City, CA) for 30 min. The tone and shock started at 60 s and repeats every 5 min. The shock was delayed by 1 second than the tone. The shock current was 300 µA with duration of 5 seconds. After 24 hours, the mouse was put into the cage again only with tone for 5 min. The monitoring video was recorded by a camera and the time of freezing after tone was calculated. The percentage of freezing time in 60 seconds was calculated.

Step through test was performed at 14 days after tMCAO. At the first day of the test, a mouse was put into the light space of smart cage (AfaSci Research Laboratories) with an electric stimulator at the base. The mouse was received an electric shock once it stepped into the dark box. After 24 hours, the mouse was put into the smart cage again without electric stimulation and monitored for 10 min. The trace was recorded by the infrared detector and analyzed by the smart cage software.

Measurement of brain infarct and atrophy volumes

Mice were sacrificed at 3 or 14 days after tMCAO. Mouse brains were cut into a series of 20 µm thick coronal sections, followed by cresyl violet staining (Sigma, St. Louis, MO). Infarct and atrophy volumes were calculated by NIH Image*J* software (National Institutes of Health, Bethesda, MD) as described previously.[26]

Immunofluorescence staining

Brain slices or cultured cells were fixed with methanol and blocked with diluted donkey serum (Jackson ImmunoResearch, West Grove, PA). Slices were incubated with primary antibodies of CD31 (1:300, R&D system, Minneapolis, MN), Ki67 (1:200, Abcam, Cambridge, UK), β-catenin (1:100, Abcam), GFAP (1:500, Millipore, Bedford, MA), NeuN (1:50, Millipore), myelin basic protein (MBP, 1:200, Abcam) and NG2 (1:200, Millipore). After rinsing with PBS, brain slices were incubated with the fluorescence conjugated second antibodies. Immunofluorescence photos were collected by a confocal microscope (Leica, Solms, Germany).

$CD31^+$ blood vessel number, vessel branch number, and number of $Ki67/CD31^+$ cell in the perifocal region were used to determine angiogenesis and vessel remodeling. For the quantification of MBP, two fields in the ischemic striatum area for each slice were randomly collected and analyzed with Image*J* software (National Institutes of Health, Bethesda, MD) for mean integrated density analysis.

Synchrotron radiation (SR) angiography

The microvessel density of mice was assessed in living mice using SR angiography at the Shanghai Synchrotron Radiation Facility. Briefly, the X-ray energy was 33.3 keV. An X-ray complementary metal

oxide semiconductor with a resolution of 6.5 μm/pixel (Hamamatsu Ltd., Hamamatsu City, Japan) was used to record high-resolution real-time angiographic images. A total of 80 μl of nonionic iodine contrast agent (350 mg I/ml, Omnipaque, GE, Shanghai, China) was injected with a syringe pump through the external carotid artery at a rate of 2 ml/min.

Imaging procedures have been described previously.[27,28] Perfused vessels were identified from original SR angiography images by a short program written in Matlab (MathWorks, Natick, MA, USA).[27] The vessel density was defined as the percentage of pixels of vessels in total pixels of each selected area.

Blood-brain barrier permeability assay

The leakage of IgG was detected to assess the blood-brain barrier permeability which indicated the vascular maturity. Briefly, brain slices were incubated with Universal ABC Kit (Vector Labs, Burlingame, CA) and the immunoreactivity was visualized by DAB reagents (Vector Labs, Burlingame, CA). After that, slices were counterstained with hematoxylin. Three fields along the ischemic area for each slice were randomly collected and analyzed with Image*J* software for integrated density analysis.

Western blot analysis

Western blot was performed as described previously.[25] Briefly, the membranes were incubated with primary antibodies against MBP (1:1000, Abcam), Wnt7a (1:500, Abcam), β-catenin (1:500, Abcam), VEGF (1:500, Abcam), β-actin (1:1000, Abcam) and GAPDH (1:1000, Abcam) overnight at 4 °C. After washing with TBST buffer, the membranes were incubated with HRP-conjugated secondary antibody.

OPC migration assay

Migration assay was performed as previously described.[29] Briefly, the migration test was performed in 24 mm transwell with 8.0 μm pore polycarbonate membrane inserts (Corning). The transwell chambers were coated with PDL for 12 hours. Human umbilical cord vein cells (HUVECs) were seeded at a density of 2×10^5 cells per well in 6-well plates. After 24 hours, the cultured medium was changed with endothelial cell medium (ECM, ScienCell, Carlsbad, CA) with or without β-catenin inhibitor (XAV-939, 1 μM, MCE, Monmouth Junction, NJ). XAV-939 (1 μM) was dissolved in ECM in 37 °C for 24 hours as well. Then, conditioned medium (CM) of HUVEC, CM of HUVEC + XAV-939 and ECM + XAV-939 were collected after 24 hours. In the lower compartment, one of the following media was added: 500 μl ECM (control), 350 μl ECM + 150 μl CM of HUVEC, 350 μl ECM + 150 μl CM of HUVEC + XAV-939 and 500 μl ECM + XAV-939. OPCs (2×10^5 per chamber) suspended in growth factor-free Neurobasal-A were added to the upper chamber. After 12 and 24 hours, chambers were stained with crystal violet (Beyotime) for 5 min. The number of OPCs that migrated to the lower membrane surface were counted manually in 5 random fields, and 4 chambers were counted for each group.

Wnt7a siRNA interference in OPCs

Sequences of interfering siRNA segments were as follows: 5-GCCUUCACCUAUGCAAUUATT-3. Non-targeting siRNA with scramble served as a negative control (NC). Sequences of NC were as follows: 5-UUCUCCGAACGUGUCACGUTT-3.

OPCs were seeded at a density of 1×10^6 cells per well in 6-well plates. After 24 hours, the culture medium was collected. Twenty μM FAM-siRNA (8 μl, Genepharma, Shanghai, China) and 3.75 μl Lipofectamine® 3000 (Invitrogen) were each diluted by 125 μl Opti-MEM (Gibco). Diluted siRNA and Lipofectamine® 3000 were mixed and added into the 1750 μl culture medium of OPCs. After 6 hours of interference, we detected the green fluorescence of FAM-siRNA in the cells. After 24 hours of interference, we changed new culture medium. And after 48 hours of interference, the CM and cell proteins of three groups (Blank, NC and siRNA) were collected.

Proliferation assay

HUVECs were isolated according to the protocol previously.[30] The umbilical cord of newborn was put into sterile PBS. The umbilical cord was filled with 0.25% trypsin, and digested at 37 °C for 10 min. The digestive fluid of umbilical vein was collected, and centrifuged at 250 *g* for 5 min. Then, the cells were resuspended with ECM (Sciencell, San Diego, CA), and seeded in the plate.

HUVECs were seeded at a density of 1×10^5 cells per well in 6-well plates and cultured for 24 hours. The cells were cultured with 70% ECM + 30% Neurobasal-A (control cultured medium, CON), 70% ECM + 30% CM of OPC, 70% ECM + 30% CM of OPC transfected by negative control siRNA (CM of NC), 70% ECM + 30% CM of OPC transfected by Wnt7a siRNA (CM of SI), 70% ECM + 30% CM of OPC plus XAV-939 (1 μM, MCE) (CM of OPC + XAV939) and 70% ECM + 30% Neurobasal-A plus Wnt7a protein (50 ng/mL, R&D system) (Wnt7a) for 24 hours.[16,31,32] Then the cells were collected for

β-catenin assay using western blot and meanwhile the cells seeded on the coverslips were incubated with Ki67 (1:200, Abcam) and CD31 (1:300, R&D system). The number of Ki67/DAPI$^+$ cells was counted manually in seven random fields.

HUVEC tube formation assay

The tube formation assay of HUVEC was performed as previously reported.[28] Briefly, 50 µl matrigel (BD Biosciences, Franklin Lakes, NJ) was added into 96-well plate and incubated at 37 °C for 30 min. HUVECs (2×10^4) were suspended in 70 µl ECM (Sciencell) and seeded in the matrigel-coated plate. CM (30 µl) was added into the 6 groups respectively as described in the proliferation experiment. After culturing for 3 hours, the tube images were captured by a microscope (Leica, Solms, Germany). The tube number and length were measured with Image*J* software (National Institutes of Health).

Statistical analysis

Sample size was determined according to our previous publications for similar outcomes.[24,25,33] Sample size was estimated using a type I error rate of 0.05 and a power of 0.8 on a 2-sided test by power analysis. Analysis was performed by SPSS. Kolmogorov-Smirnova normal test was used for data distribution test first. Multiple comparisons were analyzed using one-way ANOVA followed by Tukey's post-hoc test for normally distributed data. For non-normal continuous variables, the Mann-Whitney U test was applied. Data were expressed as mean ± SD. A probability value less than 0.05 was considered significant.

Results

OPC isolation, identification and transplantation

Cultured OPCs showed a multipolar morphology under phase contrast microscope (Figure 1(a)). To identify the culture purity, we used PDGFR-α and NG2 as markers of OPCs. Immunofluorescent staining results showed that the percentage of PDGFR-α$^+$cells was 91.60% and the percentage of NG2$^+$ cells was 93.82% (Figure 1(b) and (c)). Besides, the percentage of GFAP$^+$ and Iba-1$^+$ cells was 2.71% and 3.76%, respectively. No cells expressed oligodendrocyte marker MBP and neuron marker NeuN (Suppls. 1(a) to (d)). To track the cells after transplantation, we labeled OPCs with CFDA-SE. The results suggested that transplanted cells still survived at 28 days after tMCAO (Figure 1(d) and (e)).

OPC transplantation improved neurological outcomes and attenuated brain atrophy volume after tMCAO

The mNSS was used to evaluate the neurological function. OPC transplantation significantly ameliorated

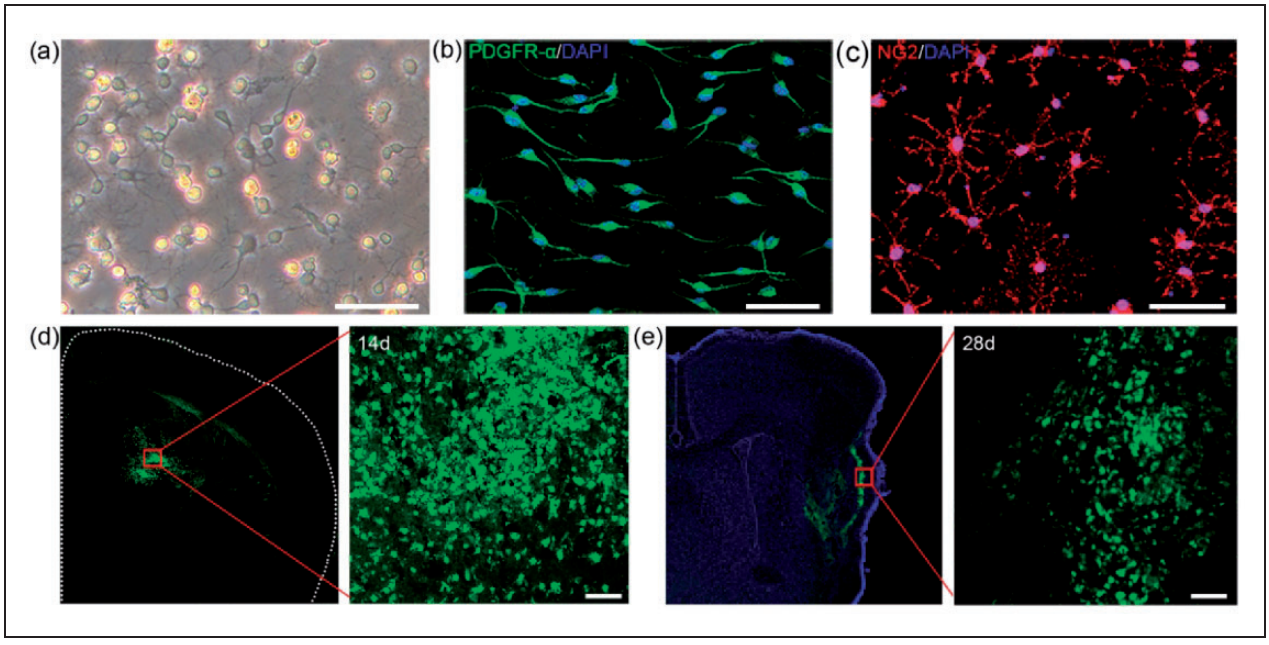

Figure 1. OPC isolation, identification and injection. (a) Morphology of cultured cells under phase contrast microscope. (b–c) Representative image of PDGFR-α (b) and NG2 (c) in cultured cells. (d–e) Survival of OPCs after injection. Green fluorescent OPCs (CFDA-SE stained) were located in the ischemic hemisphere at 14 and 28 days after tMCAO. Scale bar = 50 µm.

neurological deficits at 7 and 14 days after tMCAO (Figure 2(a), $p < 0.05$). Rotarod tests indicating motor function showed that the time staying on the rotarod was prolonged in OPC-treated mice compared to PBS-treated mice at 7 and 14 days after tMCAO (Figure 2(b), $p < 0.05$).

Fear conditioning test and step through test were used to evaluate the cognitive function at 14 days after tMCAO. In the fear conditioning test, the freezing time was longer in OPC treated mice compared with control (PBS) mice (Figure 2(c), $p < 0.05$). Step through test showed that OPC transplantation decreased the dark zone time and dark zone entries compared to the control (Figure 2(d), $p < 0.05$). Transplanted OPCs ameliorated the cognitive damage after tMCAO.

The brain infarct and atrophy volumes were evaluated by cresyl violet staining. Results showed that the brain infarct and atrophy volumes were significantly smaller in OPC treated mice compared to the control mice after tMCAO (Figure 2(e) and (f), $p < 0.05$).

OPC transplantation promoted functional angiogenesis in tMCAO mice

OPC transplantation increased the $CD31^+$ microvessels number and the vessel branch number (Figure 3(a), $p < 0.05$). In addition, the number of $CD31^+/Ki67^+$ cells was also increased in the peri-infarct region of OPC transplanted mice at 14 days after tMCAO compared to the control mice (Figure 3(b), $p < 0.05$). These results indicated that OPC transplantation promoted angiogenesis after tMCAO. To further examine the post-ischemic angiogenesis was functional, SR angiography was performed at 14 days after tMCAO. More microvessels in the peri-infarct region were observed in the OPC treated mice compared to the control mice (Figure 3(c), $p < 0.05$), indicating that the OPC transplantation induced newly formed microvessels were functional. Finally, IgG protein extravasation was measured to evaluate the vascular maturity of the new vessels. IgG staining displayed that less IgG protein leaked into the brain parenchyma in the OPC treated mice

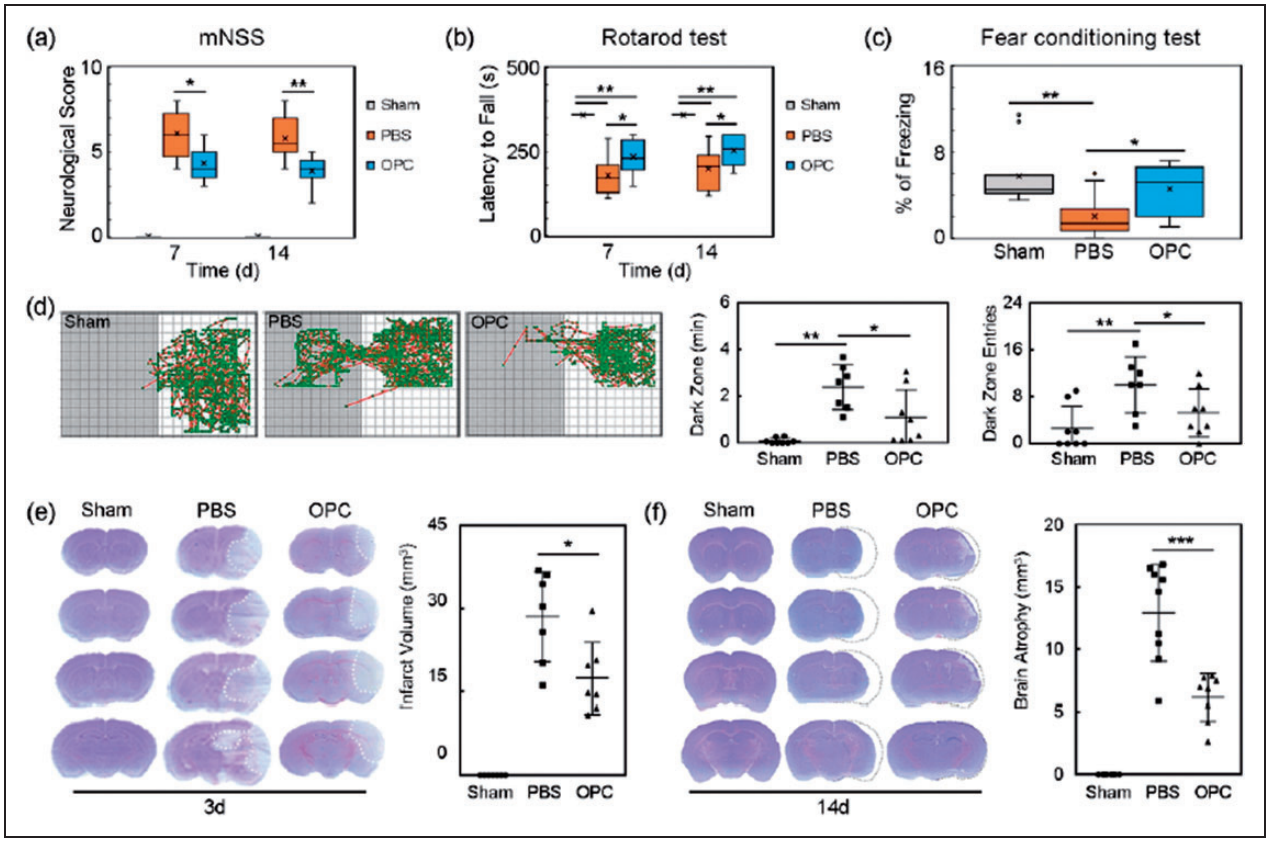

Figure 2. OPC transplantation improved neurological outcomes and reduced brain atrophy volume in ischemic mice. (a–c) Quantifications of the neurological score, time stay on the rotarod and fear conditioning test in sham, PBS and OPC groups at 7 and 14 days after tMCAO. N = 9–11 per group. (d) Trace pictures and the scatter plots of step through test showed that the dark zone time and dark zone entries. N = 7–8 per group. (e) Cresyl violet staining showed the brain infarct volume at 3 days after tMCAO. N = 7–8 per group. (f) Cresyl violet staining showed the brain atrophy volume at 14 days after tMCAO. N = 8–9 per group. Data are mean ± SD, $*p < 0.05$, $**p < 0.01$, $***p < 0.001$.

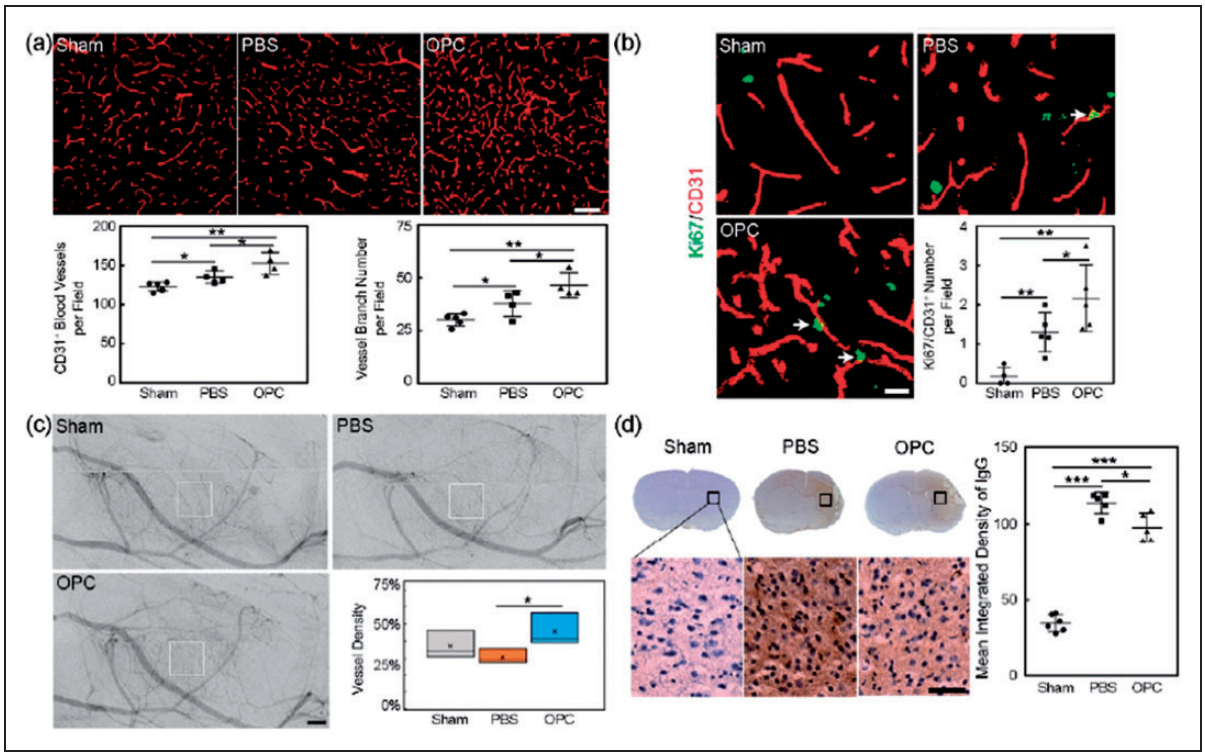

Figure 3. OPC transplantation promoted angiogenesis in ischemic mice. (a) Representative images of $CD31^+$ microvessels in peri-infarct region and bar graphs of the $CD31^+$ microvessels number and the vessel branch number in sham, PBS and OPC groups at 14 days after tMCAO. Scale bar = 100 μm, n = 4 per group. (b) Representative images of CD31 (red) and Ki67 double (green) positive cells in peri-infarct region at 14 days after tMCAO. Scale bar = 50 μm, n = 4 per group. (c) SR angiography showed microvessels in the peri-infarct region at 14 days after tMCAO. Scale bar = 500 μm, n = 3 per group. (d) IgG staining at 14 days after tMCAO. Bar graph showed the quantification of leaked IgG protein. Scale bar = 25 μm, n = 5 per group. Data are mean ± SD, $*p < 0.05$, $**p < 0.01$, $***p < 0.001$.

compared to the control (Figure 3(d), $p < 0.05$). Our result indicated that OPC transplantation promoted the functional angiogenesis after tMCAO.

OPC transplantation promoted the white matter repair after tMCAO

Immunofluorescent images showed that OPC transplantation increased the intensity of MBP in the peri-infarct region at 14 days after tMCAO (Figure 4(a), $p < 0.01$). Western blot result showed that the MBP expression was increased in OPC treated mice compared to the control (Figure 4(b), $p < 0.01$), suggesting that OPC transplantation promoted the white matter repair. We also found that the transplanted OPCs did not express MBP at 3 days after tMCAO, few transplanted OPCs expressed MBP at 14 days after tMCAO (Figure 4(c)). Most transplanted cells sustained expression of NG2 at 14 days after tMCAO (Figure 4(c)). At 28 days after tMCAO, the transplanted cells expressed MBP around the myelin. But some transplanted cells still expressed NG2 (Figure 4(d)).

Wnt/β-catenin pathway was involved in angiogenesis induced by OPC after tMCAO

OPCs can increase Wnt7a expression to promote the angiogenesis during development.[16] To examine whether Wnt7a was involved in angiogenesis after OPC transplantation, we examined the level of Wnt7a using Western blot analysis. The result showed that Wnt7a expression increased in the ipsilateral brain of OPC treated mice compared to the control at 14 days after tMCAO (Figure 5(a), $p < 0.05$). Meanwhile, OPC transplantation increased β-catenin expression in the ipsilateral hemisphere compared to the control (Figure 5(b), $p < 0.01$). Immunofluorescent results indicated that β-catenin was mainly expressed in the endothelial cells. No β-catenin expression was found in astrocytes and neurons (Figure 5(d)). We also examined whether vascular endothelial growth factor (VEGF) was involved in angiogenesis induced by exogenous OPC transplantation. The result showed that there was no difference between OPC treated mice and the control mice (Figure 5(c), $p > 0.05$).

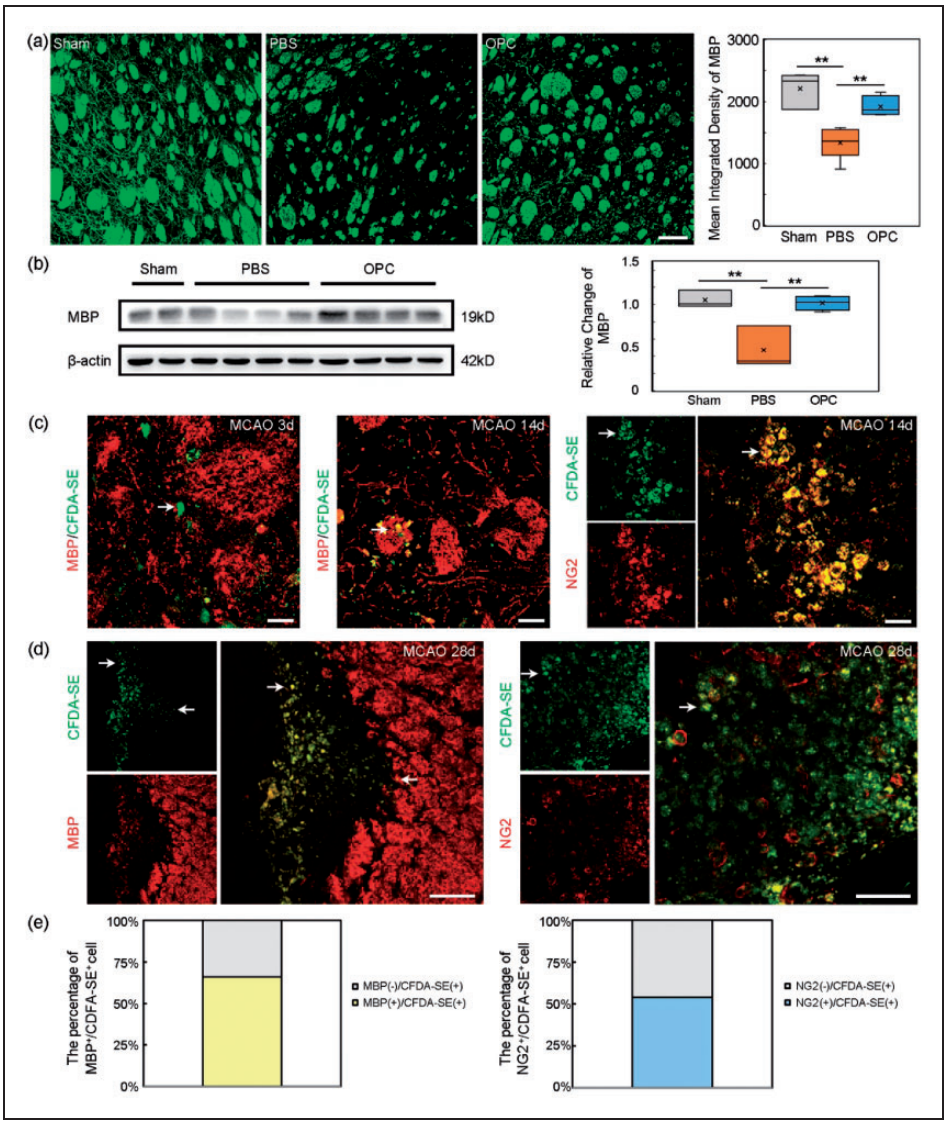

Figure 4. OPC transplantation increased MBP expression in ischemic mice. (a) Immunofluorescent images of MBP (red) and bar graph of MBP quantification in peri-infarct region in sham, PBS and OPC groups at 14 days after tMCAO. Scale bar = 100 μm. N = 4 per group. (b) The Western blot result of MBP at 14 days after tMCAO. N = 4 per group. (c) The transplanted OPCs (green, CFDA-SE stained) did not express MBP (red) at 3 days after tMCAO while some transplanted OPCs (green) expressed MBP (red) at 14 days after tMCAO. The transplanted cells (green) still expressed NG2 (red) at 14 days after tMCAO. White arrows indicated the transplanted cells. Scale bar = 25 μm. (d) The transplanted OPCs (green) expressed MBP (red) at 28 days after tMCAO. And some transplanted cells (green) still expressed NG2 (red) at 28 days after tMCAO. White arrows indicated transplanted cells. Scale bar = 100 μm. (e) The percentage of CFDA-SE cell expressing MBP and the percentage of CFDA-SE cell expressing NG2. Data are mean±SD, $^{**}p < 0.01$.

Inhibition of Wnt/β-catenin pathway reversed the beneficial role of OPCs in HUVECs

To demonstrate OPCs derived Wnt7a acting on endothelial β-catenin participated in angiogenesis induced by OPC transplantation, we knocked down the Wnt7a in OPCs or inhibited β-catenin by XAV939 to check their effects on HUVECs. After 6 hours of siRNA transfection, the Wnt7a FAM-siRNA got into the cell body of the cultured OPCs (Suppl. 2a). Western blot result showed the Wnt7a siRNA knocked down the Wnt7a expression in cultured OPCs successfully (Suppl. 2 b, $p < 0.001$). CM of OPC, CM of OPC transfected by negative control siRNA (CM of NC) and Wnt7a protein increased β-catenin expression in the HUVECs compared to the control. But CM of OPC transfected by Wnt7a siRNA (CM of SI) and CM of OPC + XAV939 deceased β-catenin expression in the HUVECs compared to CM of OPC (Figure 6(a), $p < 0.01$). Ki67/CD31/DAPI staining showed CM of

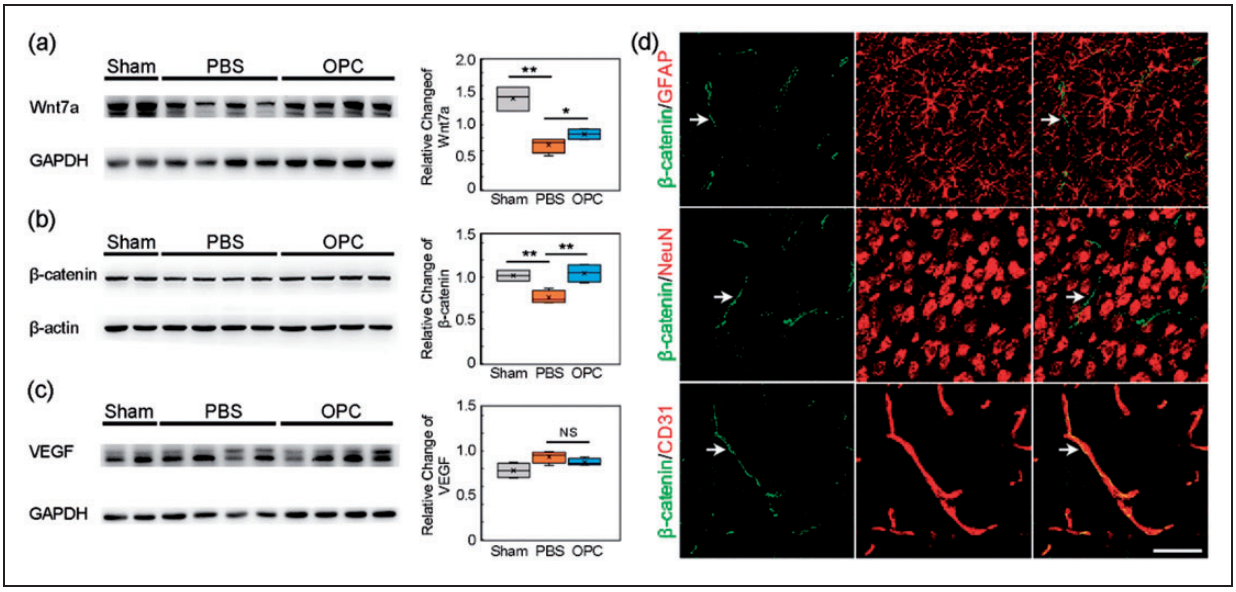

Figure 5. Wnt/β-catenin pathway was involved in angiogenesis induced by OPC transplantation after tMCAO. (a) Western blot of Wnt7a expression in sham, PBS and OPC groups at 14 days after tMCAO. (b) Western blot of β-catenin expression. (c) Western blot of VEGF expression. (d) Immunofluorescent images of β-catenin (green)/GFAP (red), β-catenin (green)/NeuN (red) and β-catenin (green)/CD31 (red). White arrows indicated β-catenin expression. Scale bar = 50 μm. Data are mean ± SD, n = 4 per group, *$p < 0.05$, **$p < 0.01$, NS>0.05.

OPC and Wnt7a protein promoted HUVEC proliferation. The knockdown of Wnt7a or inhibition of β-catenin attenuated the proliferation of HUVEC (Figure 6(b), $p < 0.001$). CM of OPC and Wnt7a protein increased the tube number per field and fold change of tube length of HUVECs. The knockdown of Wnt7a or inhibition of β-catenin reversed the HUVEC tube-formation (Figure 6(c), $p < 0.05$).

OPC migration depended on the endothelial β-catenin

In order to explore whether endothelial cells could affect the ability of OPC migration, we performed a transwell assay. Results showed that CM of HUVEC increased the number of migrated OPCs during 12 and 24 hours compared to the control, indicating CM of HUVEC promoted the OPC migration (Figure 6(d), $p < 0.05$). While HUVECs were treated with the β-catenin inhibitor (XAV-939), CM of HUVEC plus XAV-939 could block the OPC migration in CM of HUVEC.

Inhibition of wnt/β-catenin pathway reversed the beneficial role of OPCs in mice

In order to verify the Wnt/β-catenin pathway, we used β-catenin inhibitor XAV-939 *in vivo* and found that the beneficial role of OPC transplantation was reversed (Figure 7, $p < 0.05$). The mNSS which indicated neurological deficits was increased in XAV-939 group at 7 and 14 days after tMCAO (Figure 7(a), $p < 0.05$). The time staying on the rotarod of rotarod tests which indicated motor function was shortened in OPC + XAV-939 group compared to OPC group at 7 and 14 days after tMCAO (Figure 7(b), $p < 0.05$). XAV-939 decreased the $CD31^+$ microvessels number (Figure 7 (c), $p < 0.05$).

Discussion

In the present study, we found that OPC transplantation promoted post-ischemic functional angiogenesis and increased MBP expression, improved neurobehavioral outcomes and alleviated cognitive defects after tMCAO. Our study also provided a molecular mechanism of exogenous OPC transplantation in ischemic stroke.

Many types of stem cells have the potential for the treatment of ischemic stroke.[34] White matter is affected in most cases of human stroke.[3] Oligodendrocytes and OPCs are highly sensitive to ischemia, and ischemia causes the white matter injury and OPC death. Therefore, we chose OPC transplantation to promote white matter repair after ischemic stroke. In our previous study, OPC transplantation showed protective effect on blood-brain barrier permeability in the early phase of tMCAO.[14] In this study we further demonstrated that OPC transplantation promoted angiogenesis, which decreased brain infarct volume in the early

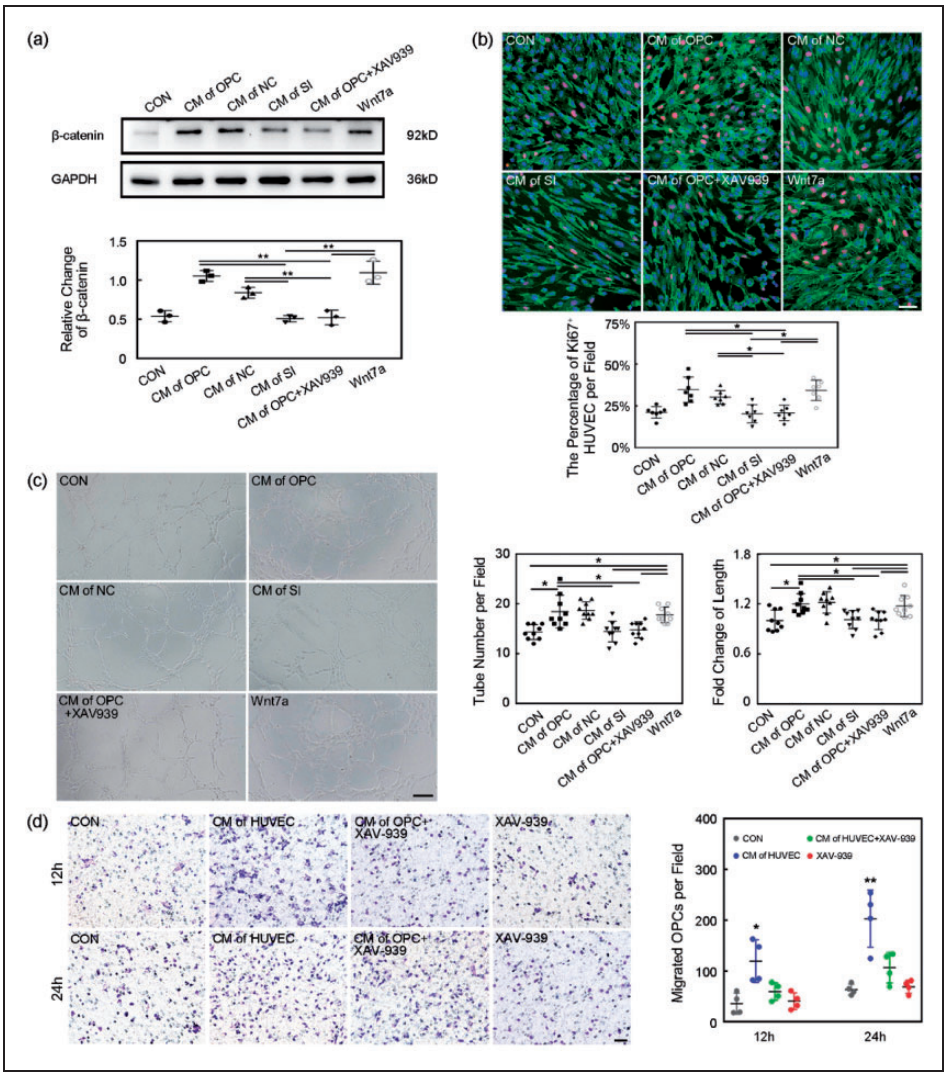

Figure 6. Endothelial β-catenin inhibition blocked beneficial role of OPCs in HUVECs. (a) Western blot of β-catenin expression of HUVECs in CM, CM of OPC, CM of NC, CM of SI, CM of OPC+XAV939 and CM+Wnt7a groups. Data are mean±SD, n = 3 per group, $^{**}p < 0.01$. CON: control, only with cultured medium; CM of OPC: conditioned medium of OPC; CM of NC: conditioned medium of OPC transfected by negative control siRNA; CM of SI: conditioned medium of OPC transfected by Wnt7a siRNA; CM of OPC+XAV939: conditioned medium of OPC+XAV939; Wnt7a: cultured medium+Wnt7a protein. (b) Representative images and bar graph of Ki67 (red)/CD31 (green)/DAPI (blue) staining showed the proliferation of HUVECs. Scale bar = 50 μm. Data are mean ± SD, n = 7 per group, $^{*}p < 0.05$. (c) Representative images and bar graphs showed the tube-formation of HUVECs. Scale bar = 200 μm. Data are mean±SD, n = 9 per group, $^{*}p < 0.05$. (d) The migration ability of OPCs was assessed by transwell *in vitro*. Images showed the migrated OPCs during 12 and 24 hours. Scale bar = 50 μm, n = 4 per group. Data are mean±SD, $^{*}p < 0.05$, $^{**}p < 0.01$, as compared to the CON, CM of HUVEC+XAV-939 and XAV-939 groups. CON: control, cultured medium without OPCs; CM of HUVEC: conditioned medium of HUVECs; CM of HUVEC+XAV-939: conditioned medium of HUVECs treated with XAV-939; XAV-939: cultured medium only with XAV-939.

phase of tMCAO, decreased brain atrophy volume and improved stroke outcomes in the recovery period, suggesting as a stem cell, OPC might have multiple functions during ischemic brain injury. The initial goal of stem cell therapy is to replace the damaged tissue by cell replacement. When neural stem cells are transplanted into the brains of ischemic adult and aged rats, only 20% differentiate into Tuj-1^{+} neurons, and more than 75% differentiate into GFAP^{+} astrocytes.[35] To date, there is no clear evidence that mesenchymal stem cells differentiate into mature neurons with electrophysiological properties in the stroke model. Another possible role of stem cells in the therapy is that grafted stem cells could directly release growth and trophic factors, or promote the release of such factors from host brain cells. Our results indicated that the effect of OPC transplantation is mainly through paracrine.

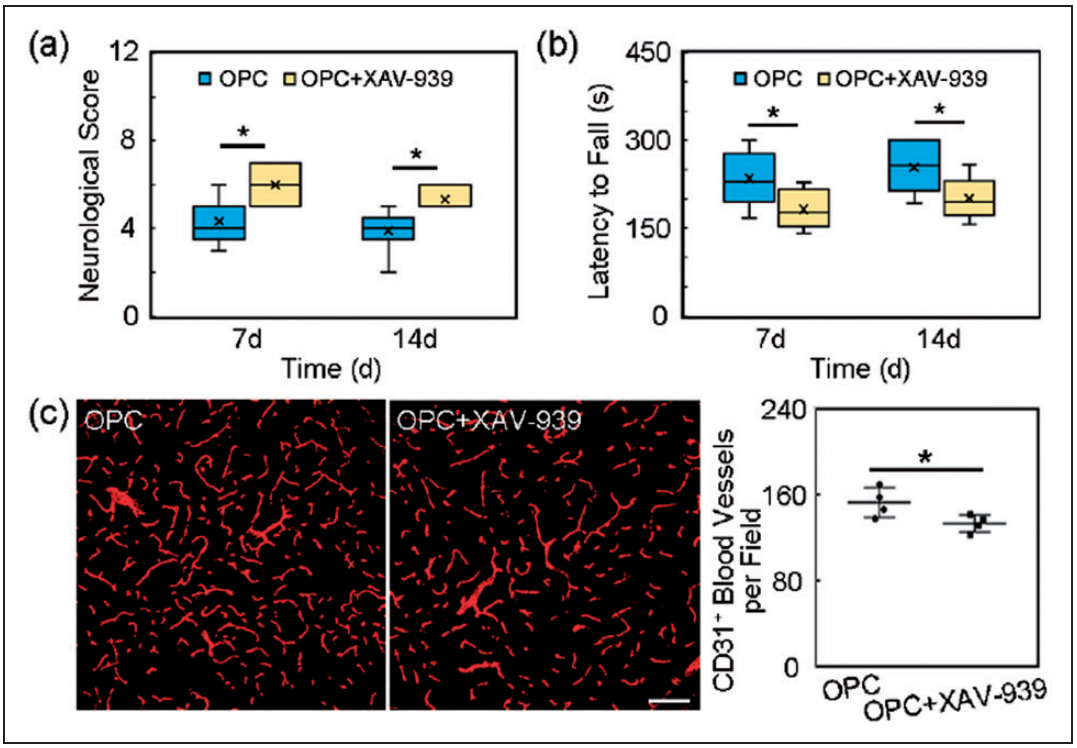

Figure 7. Inhibition of β-catenin reversed the beneficial role of OPCs *in vivo*. (a) Quantification of the neurological score in the OPC and OPC+XAV-939 groups at 7 and 14 days after tMCAO. N = 6-8 per group. (b) Quantification of the time stay on the rotarod in the OPC and OPC+XAV-939 groups at 7 and 14 days after tMCAO. N = 6-8 per group. (c) Representative images of CD31+ microvessels in the peri-infarct region and bar graphs of the CD31+ microvessels number in the OPC and OPC+XAV-939 groups at 14 days after tMCAO. Scale bar = 100 μm. N = 4 per group. Data are mean±SD, $^*p < 0.05$.

Post-ischemic angiogenesis contributes to improved neurological recovery by promoting brain tissue repair, vascular remodeling, and plasticity.[36] Angiogenesis appears by days 4 to 7 in peri-infarct regions and has been purported to be associated with neurogenesis. Circle of Willis and pial collateral vasculature provide protection from significant focal ischemic injury. Capillary density is important to the processes of recovery and limitation of injury.[37] Permanent MCAO could induce neo-collateral formation which caused a decrease in infarct volume.[38] Although restoration of the blood supply provides oxygen, nutrients and trophic factors, aberrant growth of new capillaries poses the risk for immature vessel formation that may enhance blood–brain barrier damage. But pre-clinical research indicated that restoration of the vascular anatomy and blood flow increases the neuronal and functional recovery following stroke.[39]

Studies reported that OPCs could promote white matter angiogenesis in postnatal mice.[40] Our study indicated that OPCs could survive at least for 4 weeks post intracerebral transplantation. OPC transplantation promoted functional angiogenesis in the peri-infarct area after ischemic stroke. Angiogenesis resulted in brain microvasculature changes following cerebral ischemia which promoted tissue repair and reduced brain atrophy. First, OPC transplantation increased the number of $CD31^+$ microvessels in the peri-infarct area. Second, SR angiography indicated that OPC transplantation induced the functional microvessel formation around the ischemic area. Third, IgG leakage indicated that OPC transplantation promoted the maturity of the newly formed microvessels. OPCs were a source of Wnt7a, which served as the dominant ligands acting on Frizzled receptors of brain endothelial cells and then activated β-catenin for endothelial proliferation and tight junction formation.[15] Furthermore, our results supported that OPC transplantation improved angiogenesis through Wnt/β-catenin signaling after tMCAO. OPC transplantation increased the levels of Wnt7a and β-catenin compared to the control which suggested that OPC transplantation promoted angiogenesis by activating the Wnt/β-catenin pathway. Silencing the expression of Wnt7a in OPCs with siRNA and inhibition of β-catenin by XAV-939 in HUVECs could block the promotion of proliferation and tube formation of HUVECs induced by CM of OPC. Besides, endothelial β-catenin facilitated OPC migration.

Recent studies showed that cell-cell crosstalk between OPCs and endothelial cells played a critical role in angiogenesis. The conditional knockout of Wnt in OPCs resulted in dampened compensatory angiogenesis in cerebral white matter of neonatal mice subjected to hypoxia.[41,42] Our results supported that Wnt signal derived from transplanted OPCs could promote angiogenesis in the ischemic perifocal region in adult rodents. Under the SR angiography, we further found that these newly formed microvessels were functional during tMCAO, and Wnt7a secreted from OPCs acted on β-catenin on the endothelial cell side could promote angiogenesis. In addition, our current study focused on the motor and cognitive recovery from exogeneous OPC treatment after tMCAO and the exploration of preliminary molecular mechanism.

Although there was no direct evidence to link the OPC-promoted angiogenesis with white matter integrity, we transplanted OPC into the striatum, which consisted of lots of white matter fiber bundles and was distinctly damaged in the tMCAO mouse brain. Previous study indicated that CXCR4 of OPCs binding the ligand CXCL12, which was expressed by the endothelial cells mediated the OPC migration along vasculature during the development, and the migration was disrupted in mice with defective vascular architecture.[43,44] Our study also demonstrated that co-culture of endothelial cells could promote OPC migration *in vitro*. Angiogenesis participated in the brain plasticity and functional recovery during chronic phase of ischemic stroke. Our results showed that OPC transplantation promoted angiogenesis and functional recovery after tMCAO. The β-catenin inhibitor decreased HUVEC proliferation *in vitro* and blocked angiogenesis *in vivo*, which aggravated neurobehavioral outcomes after tMCAO. Nevertheless, we assumed that the improved white matter integrity in the OPC-treated tMCAO mice most likely depended on enhanced angiogenesis.

Since myelin maintains axon integrity and provides trophic support for axons, enabling rapid transmission of action potentials through salutatory conduction,[43] myelin destruction after white matter injury resulted in severe cognitive dysfunction.[3] OPCs are canonical cells to differentiate into oligodendrocytes and participate in remyelination after ischemic injury.[45] White matter injury after stroke is characterized by the death of oligodendrocytes and OPCs and profound loss of myelin integrity. And the death of OPCs results in inadequate remyelination. The white matter integrity improvements after stroke may be achieved by protecting white matter components against ischemic injury and/or enhancing white matter repair and regeneration.[46] Our results supported that OPC transplantation contributed to the white matter repairing and remodeling, as well as cognitive recovery by producing trophic factors after tMCAO. First, although some transplanted OPCs could differentiate to the mature oligodendrocytes and involve in the myelin repairing and remodeling, a mount of transplanted cells kept the progenitor cell properties and did not directly participate in remyelination. However, only immunostaining figures were not enough to verify transplanted OPCs directly participated in remyelination. The time lapse experiment to chase the differentiation of transplanted OPCs after tMCAO is needed in the future. Second, angiogenesis induced by OPC transplantation could facilitate the OPC migration and re-myelination after ischemic brain injury. Third, endothelial cells could promote the OPC migration *in vitro*, and endothelial β-catenin was involved in this process. Fourth, OPC transplantation increased MBP expression for remyelination.

Our results demonstrated a novel pathway that Wnt7a from oligodendrocyte precursor cells acting on endothelial β-catenin promoted angiogenesis and improved neurobehavioral outcomes, which facilitated white matter repair and remodeling during ischemic stroke.

Funding

The author(s) disclosed receipt of the following financial support for the research, authorship, and/or publication of this article: This study was supported by grants from the National Natural Science Foundation of China (82001228, LPW; 81771251, GYY; 81771244, ZZ; 819741798, ZZ; 81870921, YW; 81801170, YHT; 82071284, YHT), and the National Key Research and Development Program of China (2016YFC1300600).

Declaration of conflicting interests

The author(s) declared no potential conflicts of interest with respect to the research, authorship, and/or publication of this article.

Authors' contributions

LPW: conception and design, provision of study material, collection and assembly of data, and manuscript writing; JP and YL: provision of study material and data analysis; JG, CL and PZ: collection and assembly of data; LYZ and YHT: data analysis and interpretation; YW, ZZ, and GYY: financial support and manuscript writing.

Supplemental material

Supplemental material for this article is available online.

References

1. Strong K, Mathers C and Bonita R. Preventing stroke: saving lives around the world. *Lancet Neurol* 2007; 6: 182–187.

2. Benjamin EJ, Blaha MJ, Chiuve SE, et al.; American Heart Association Statistics Committee and Stroke Statistics Subcommittee. Heart disease and stroke statistics-2017 update: a report from the American Heart Association. *Circulation* 2017; 135: e146–e603.
3. Wang Y, Liu G, Hong D, et al. White matter injury in ischemic stroke. *Prog Neurobiol* 2016; 141: 45–60.
4. Cai M, Zhang W, Weng Z, et al. Promoting neurovascular recovery in aged mice after ischemic stroke – prophylactic effect of omega-3 polyunsaturated fatty acids. *Aging Dis* 2017; 8: 531–545.
5. Zamroziewicz MK, Paul EJ, Zwilling CE, et al. Predictors of memory in healthy aging: polyunsaturated fatty acid balance and fornix white matter integrity. *Aging Dis* 2017; 8: 372–383.
6. Ho PW, Reutens DC, Phan TG, et al. Is white matter involved in patients entered into typical trials of neuroprotection? *Stroke* 2005; 36: 2742–2744.
7. Susuki K and Rasband MN. Molecular mechanisms of node of Ranvier formation. *Curr Opin Cell Biol* 2008; 20: 616–623.
8. Li N and Leung GK. Oligodendrocyte precursor cells in spinal cord injury: a review and update. *Biomed Res Int* 2015; 2015: 235195.
9. Watzlawik J, Warrington AE and Rodriguez M. Importance of oligodendrocyte protection, BBB breakdown and inflammation for remyelination. *Expert Rev Neurother* 2010; 10: 441–457.
10. Sher F, Balasubramaniyan V, Boddeke E, et al. Oligodendrocyte differentiation and implantation: new insights for remyelinating cell therapy. *Curr Opin Neurol* 2008; 21: 607–614.
11. Fu H, Hu D, Zhang L, et al. Efficacy of oligodendrocyte progenitor cell transplantation in rat models with traumatic thoracic spinal cord injury: a systematic review and meta-analysis. *J Neurotrauma* 2018; 35: 2507–2518.
12. Chari DM and Blakemore WF. New insights into remyelination failure in multiple sclerosis: implications for glial cell transplantation. *Mult Scler* 2002; 8: 271–277.
13. Chen LX, Ma SM, Zhang P, et al. Neuroprotective effects of oligodendrocyte progenitor cell transplantation in premature rat brain following hypoxic-ischemic injury. *PLoS One* 2015; 10: e0115997.
14. Wang L, Geng J, Qu M, et al. Oligodendrocyte precursor cells transplantation protects blood-brain barrier in a mouse model of brain ischemia via Wnt/beta-catenin signaling. *Cell Death Dis* 2020; 11: 9.
15. Cho C, Smallwood PM and Nathans J. Reck and Gpr124 are essential receptor cofactors for Wnt7a/Wnt7b-specific signaling in mammalian CNS angiogenesis and blood-brain barrier regulation. *Neuron* 2017; 95: 1221–1225.
16. Yuen TJ, Silbereis JC, Griveau A, et al. Oligodendrocyte-encoded HIF function couples postnatal myelination and white matter angiogenesis. *Cell* 2014; 158: 383–396.
17. Corada M, Nyqvist D, Orsenigo F, et al. The Wnt/beta-catenin pathway modulates vascular remodeling and specification by upregulating Dll4/notch signaling. *Dev Cell* 2010; 18: 938–949.
18. Olsen JJ, Pohl SO, Deshmukh A, et al. The role of Wnt signalling in angiogenesis. *Clin Biochem Rev* 2017; 38: 131–142.
19. Arai K, Jin G, Navaratna D, et al. Brain angiogenesis in developmental and pathological processes: neurovascular injury and angiogenic recovery after stroke. *Febs J* 2009; 276: 4644–4652.
20. Hamanaka G, Ohtomo R, Takase H, et al. White-matter repair: interaction between oligodendrocytes and the neurovascular unit. *Brain Circ* 2018; 4: 118–123.
21. Percie Du Sert N, Hurst V, Ahluwalia A, et al. The ARRIVE guidelines 2.0: updated guidelines for reporting animal research. *J Cereb Blood Flow Metab* 2020; 40: 1769–1777.
22. Chen Y, Balasubramaniyan V, Peng J, et al. Isolation and culture of rat and mouse oligodendrocyte precursor cells. *Nat Protoc* 2007; 2: 1044–1051.
23. Yuan F, Chang S, Luo L, et al. cxcl12 gene engineered endothelial progenitor cells further improve the functions of oligodendrocyte precursor cells. *Exp Cell Res* 2018; 367: 222–231.
24. Geng J, Wang L, Qu M, et al. Endothelial progenitor cells transplantation attenuated blood-brain barrier damage after ischemia in diabetic mice via HIF-1alpha. *Stem Cell Res Ther* 2017; 8: 163.
25. Tang G, Liu Y, Zhang Z, et al. Mesenchymal stem cells maintain blood-brain barrier integrity by inhibiting aquaporin-4 upregulation after cerebral ischemia. *Stem Cells* 2014; 32: 3150–3162.
26. Li Y, Huang J, He X, et al. Postacute stromal cell-derived factor-1alpha expression promotes neurovascular recovery in ischemic mice. *Stroke* 2014; 45: 1822–1829.
27. Mu ZH, Jiang Z, Lin XJ, et al. Vessel dilation attenuates endothelial dysfunction following middle cerebral artery occlusion in hyperglycemic rats. *CNS Neurosci Ther* 2016; 22: 316–324.
28. Chen C, Lin X, Wang J, et al. Effect of HMGB1 on the paracrine action of EPC promotes post-ischemic neovascularization in mice. *Stem Cells* 2014; 32: 2679–2689.
29. Miyamoto Y, Yamauchi J and Tanoue A. Cdk5 phosphorylation of WAVE2 regulates oligodendrocyte precursor cell migration through nonreceptor tyrosine kinase fyn. *J Neurosci* 2008; 28: 8326–8337.
30. Jaffe EA, Nachman RL, Becker CG, et al. Culture of human endothelial cells derived from umbilical veins. Identification by morphologic and immunologic criteria. *J Clin Invest* 1973; 52: 2745–2756.
31. Huang SM, Mishina YM, Liu S, et al. Tankyrase inhibition stabilizes axin and antagonizes Wnt signalling. *Nature* 2009; 461: 614–620.
32. von Maltzahn J, Renaud JM, Parise G, et al. Wnt7a treatment ameliorates muscular dystrophy. *Proc Natl Acad Sci USA* 2012; 109: 20614–20619.
33. Huang J, Li Y, Tang Y, et al. CXCR4 antagonist AMD3100 protects blood-brain barrier integrity and reduces inflammatory response after focal ischemia in mice. *Stroke* 2013; 44: 190–197.
34. Tang YH, Ma YY, Zhang ZJ, et al. Opportunities and challenges: stem cell-based therapy for the treatment of ischemic stroke. *CNS Neurosci Ther* 2015; 21: 337–347.

35. Tang Y, Wang J, Lin X, et al. Neural stem cell protects aged rat brain from ischemia-reperfusion injury through neurogenesis and angiogenesis. *J Cereb Blood Flow Metab* 2014; 34: 1138–1147.
36. Sun P, Zhang K, Hassan SH, et al. Endothelium-targeted deletion of microRNA-15a/16-1 promotes poststroke angiogenesis and improves long-term neurological recovery. *Circ Res* 2020; 126: 1040–1057.
37. Kanazawa M, Takahashi T, Ishikawa M, et al. Angiogenesis in the ischemic core: a potential treatment target? *J Cereb Blood Flow Metab* 2019; 39: 753–769.
38. Zhang H, Rzechorzek W, Aghajanian A, et al. Hypoxia induces de novo formation of cerebral collaterals and lessens the severity of ischemic stroke. *J Cereb Blood Flow Metab* 2020; 40: 1806–1822.
39. Rust R. Insights into the dual role of angiogenesis following stroke. *J Cereb Blood Flow Metab* 2020; 40: 1167–1171.
40. Lim RG, Quan C, Reyes-Ortiz AM, et al. Huntington's disease iPSC-derived brain microvascular endothelial cells reveal WNT-mediated angiogenic and blood-brain barrier deficits. *Cell Rep* 2017; 19: 1365–1377.
41. Chavali M, Ulloa-Navas MJ, Perez-Borreda P, et al. Wnt-dependent oligodendroglial-endothelial interactions regulate white matter vascularization and attenuate injury. *Neuron* 2020; 108: 1130–1145.
42. Arai K and Lo EH. Wiring and plumbing: oligodendrocyte precursors and angiogenesis in the oligovascular niche. *J Cereb Blood Flow Metab* 2021; 41: 2132–2133.
43. Tsai HH, Niu J, Munji R, et al. Oligodendrocyte precursors migrate along vasculature in the developing nervous system. *Science* 2016; 351: 379–384.
44. Obermeier B, Daneman R and Ransohoff RM. Development, maintenance and disruption of the blood-brain barrier. *Nat Med* 2013; 19: 1584–1596.
45. Song FE, Huang JL, Lin SH, et al. Roles of NG2-glia in ischemic stroke. *CNS Neurosci Ther* 2017; 23: 547–553.
46. Dai X, Chen J, Xu F, et al. TGFalpha preserves oligodendrocyte lineage cells and improves white matter integrity after cerebral ischemia. *J Cereb Blood Flow Metab* 2020; 40: 639–655.